Available online at www.sciencedirect.com
ScienceDirect
Trans. Nonferrous Met. Soc. China 20(2010) s665−s669
Transactions of Nonferrous Metals Society of China
www.tnmsc.cn

Comparison in characterization of composite and sol-gel coating on AZ31 magnesium alloy

WANG Zhen-lin(王振林), ZENG Rong-chang(曾荣昌)

School of Materials Science and Engineering, Chongqing University of Technology, Chongqing 400050, China

Received 23 September 2009; accepted 30 January 2010

Abstract: An Al_2O_3 protective coating on magnesium alloy AZ31 was prepared by a repeated direct sol-gel process annealing at 300 ˚C and a composite coating was also deposited using Al_2O_3 particles dispersed sol followed by phosphating treatment and annealing at 300 ˚C. The morphologies, structures and critical adhesive loads as well as corrosion properties of the coatings were comparatively investigated by scanning electron microscopy (SEM), X-ray diffractometry (XRD), nanoscratch test and electrochemical measurement. The results show that the composite coating has a more uniform, crack-free layer and improved adhesion to the substrate as compared with that of the repeated direct sol-gel coating owing to its lower heat strain. The main phases in both coatings consist of γ-Al_2O_3 and δ-Al_2O_3 derived from annealed alumina sol, and the composite coating has an anticorrosion performance which is superior to that of the repeated direct sol-gel coating.
Key words: sol-gel; composite coating; magnesium alloy

1 Introduction

Magnesium and its alloys have been widely used in automobile and computer parts, aerospace components, mobile phones, sporting goods, handheld tools and household equipments due to their lightweight. Their applications are, nevertheless, still limited on account of their relatively poor corrosion resistance and wear resistance[1−2]. One of the ideal approaches to overcome the inherent drawbacks is to deposit a protective coating on magnesium alloys. The various processes include chemical conversion coating[3−4], anodizing[5], microarc oxidation[6], physical vapor deposition (PVD)[7], chemical vapor deposition (CVD)[8], ion implantation[9] and heat spraying[10]. The mentioned technologies dealing with the protection of magnesium are hard to achieve popularities on account of higher cost-to-benefit ratio or energy consumption or environmental adverse effects, and the novel surface modification by sol-gel with the virtue of being simple and cost-effective shows competitiveness to some extent[11]. It is well known that Al_2O_3 coatings have been extensively used as isolator, thermal barrier, anti-corrosion and anti-wear films[12]. The sol-gel process has been utilized to fabricate Al_2O_3[13], zirconia[14], zirconia silica[11] coatings on magnesium alloy. However, the conventional sol-gel film tends to crack if it is thicker than several micrometers. it is possible to obtain a thin and crack-free layer with thickness less than 1 μm because of the shrinkage of the coating during drying and densification the maximum coating thickness is strongly limited[15]. In view that the sol-gel based coatings are generally porous and cracky which are the main causes of degradation, the efforts have been made to minimize the shortcoming. A anti-corrosion sol-gel based Al_2O_3 coating was developed on the AZ91D magnesium alloy with phytic acid conversion coating as an interlayer to restrain corrosion activities resulting from pores and cracks of the coating[13]. The sol-gel based coatings consisting of Al_2O_3 and CeO_2 in silica matrix enhance wear resistance as well as the corrosion protection were deposited on AZ31 and AZ91D magnesium alloys[16]. The hybrid sol-gel coatings were fabricated by incorporating a corrosion inhibitor into the films[17].

For extended applications, further efforts will be focused on increasing layer thickness, the adhesion to substrate and preventing crack formation in the prepared coatings[18]. The modification to fabricate a thicker

Foundation item: Project(2005Z023) supported by the Scientific Research Initial Funding of Chongqing University of Technology
Corresponding author: WANG Zhen-lin; Tel: +86-23-68668874; Fax: +86-23-68667140; E-mail: wzl@cqut.edu.cn

protective film by sol-gel on magnesium can be realized by multiply-layers through repeated deposition. Composite alumina coatings of larger thickness can be fabricated by the sol-gel process through introducing the fillers, such as nano scaled boehmite powder[18] and calcined ceramic[19], into the gel phase. The two methodologies can effectively increase the thickness of the coating, but there are great differences in the properties of the coatings depending on the deposition processes. The objective of this study is to comparatively investigate the process and properties of the repeated direct sol-gel and the composite coatings. The alumina protective coatings were initially deposited on AZ31 magnesium alloy by a repeated direct sol-gel process, and the composite coating on the same substrate was also produced using Al_2O_3 fine particles dispersed sol followed by phosphating treatment. The coatings were characterized and the effects of the process on their properties were analyzed comparatively.

2 Experimental

The sol was prepared by hydrating aluminum isopropoxide ($Al(OC_3H_7)_3$) with distilled water in a molar ratio of 1:90 (isopropoxide to water) at about 85 ˚C with stirring for 1 h, and then the nitric acid was added into the solution to adjust the pH value to about 3. After aging for 3 h, a clear sol was consequently obtained. The resultant sol was divided into two parts designated as sol A and B.

The AZ31 magnesium alloy plates were applied as the substrates. The specimens were cut into pieces with size of 20 mm×20 mm×2 mm and their surfaces were grounded via 1 200 grit SiC paper and degreased ultrasonically in acetone and then dried with hot air. The sol A was used for preparing the sol-gel coating by dipping the pretreated magnesium alloy plate into the sol and withdrawing at a rate of about 6 cm/min. The coating was then dried for 15 min at temperature of 75 ˚C. The thicker films were produced by repeating the dipping process four times followed by thermal treatment for 10 min at 300 ˚C in a furnace. The sol B was used for producing the composite coatings. 80% Al_2O_3 (volume fraction) powders with a mean particle size of about 0.3 μm were dispersed in the sol B and the obtained blend was ultrasonically mixed for 15 min. The slurry was then coated on the pretreated magnesium alloy using a sprayer, and then the coating was baked at 75 ˚C for 15 min and was successively heat treated at 300 ˚C for 10 min, followed by spraying diluted phosphoric acid onto the coating and again heat treated at 300 ˚C for 10 min. The process flow is shown in Fig.1.

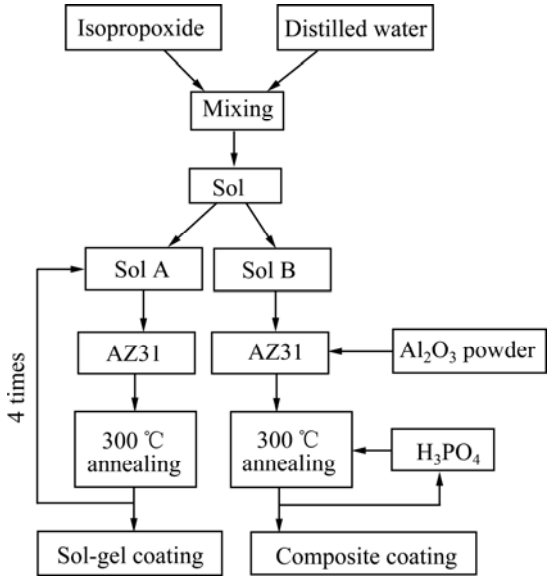

Fig.1 Flow chart for preparation of coatings on AZ31 magnesium alloy

The structures of the resultant coatings A and B were examined by X-ray diffraction (XRD) with Cu K_α radiation. The morphologies of the surfaces and cross-section were observed using JSM−6460LV scanning electron microscope (SEM). The mechanical properties of the coatings were characterized by virtue of MML Nanotest system utilizing a Rockwell diamond probe with tip diameter of 25 μm. The nanoscratch test was performed at scan velocity of 10 μm/s by linearly increasing load to 3 N with increasing velocity of 10 mN/s applied after 500 μm displacement till the total scratch length reached 3 500 μm. The electrochemical measurements were performed on a EG&G 273A type potentiostat, using Pt as auxiliary electrode, saturated calomel electrode (SCE) as reference electrode and 3.5% NaCl solution as aggressive medium. The potential was scanned from −1.8 to 0.7 V (vs SCE) at scanning rate of 0.5 mV/s.

3 Results and analysis

3.1 Morphologies of coatings

The morphologies on the surface and cross-sectional view for the repeated direct sol-gel and composite coatings are shown in Fig.2. It can be seen from Fig.2(a) that the repeated direct sol-gel coating has a dense and smooth surface but a variety of long cracks exist in the coating. From Fig.2(b), the obvious gaps among successive repeated layers can be seen, and this implies that the coating is poorly adhered to the substrate. For the composite coating as indicated in Fig.2(c), the surface is rough and slightly porous with Al_2O_3 particles bonded evenly in the matrix, no obvious cracks appear

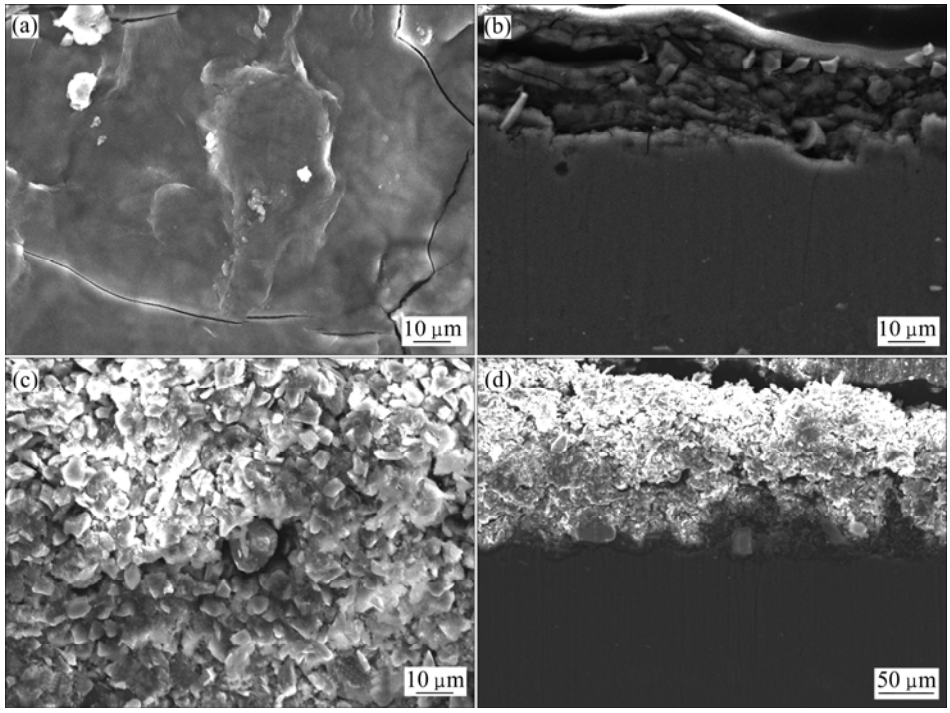

Fig.2 Morphologies of surface((a), (c)) and cross section((b), (d)) of repeated direct sol-gel coating((a), (b)) and composite coatings((c), (d))

and the coating adheres to the substrate firmly (Fig.2(d)). The repeated direct sol-gel coating tends to crack due to the presence of large strain upon heat treatment and densification. While no crack on the composite coatings develops during drying because the gel phase containing amounts of Al_2O_3 ceramic filler prevents the occurrence of great thermal strain. The cross-sectional morphologies indicate a mean thickness of approximately 30 μm for the repeated direct sol-gel (Fig.2(b)) and 120 μm for the composite coating (Fig.2(d)). The composite coating achieves a larger thickness for merely one cycle as compared with the repeated direct sol-gel process for several deposition cycles.

3.2 Structure of coatings

Fig.3 exhibits the XRD patterns of the repeated direct sol-gel and the composite coatings on AZ31 magnesium alloy. From Fig.3, the characteristic peaks of γ-Al_2O_3 and δ-Al_2O_3 observed imply the existence of crystallized γ-Al_2O_3 and δ-Al_2O_3 transferred from alumina sol annealed at 300 ˚C in the amorphous coating. The stronger and sharper diffracted peaks correspond to α-Al_2O_3 detected in the composite coating as compared with that of the repeated direct sol-gel coating, which indicates a perfectly crystallized α-Al_2O_3 phase owing to its direct introduction of Al_2O_3 ceramic particles. The composite coating is composed of large scale of α-Al_2O_3 and a small amount of γ-Al_2O_3 and δ-Al_2O_3. However, the γ-Al_2O_3 and δ-Al_2O phases in the repeated direct sol-gel coating exhibiting weak and broadened diffraction peaks are derived from poor crystallization of the gel by thermal treatment at 300 ˚C.

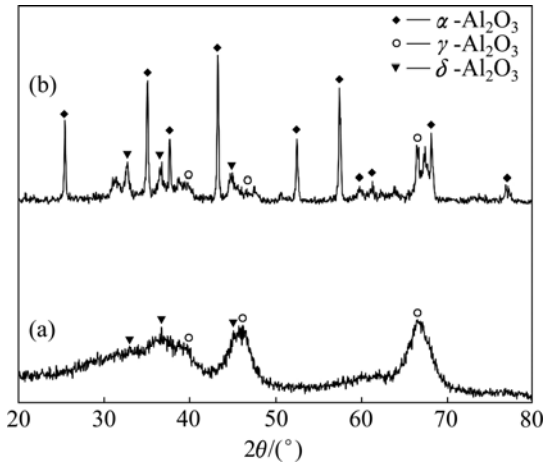

Fig.3 XRD patterns of repeated direct sol-gel(a) and composite coatings(b) on AZ31 magnesium alloy

3.3 Critical adhesive loads

The wear performances of the coatings can be investigated by means of nanoscratch tests, which can be used to measure critical load during adhesive failure of the coating/substrate system. Fig.4 illustrates the relationship among the depth, load and sliding displacement, which consists of a ramped-load scratch topography (curve 1) with a progressively increasing load from zero to the maximum value shown by a

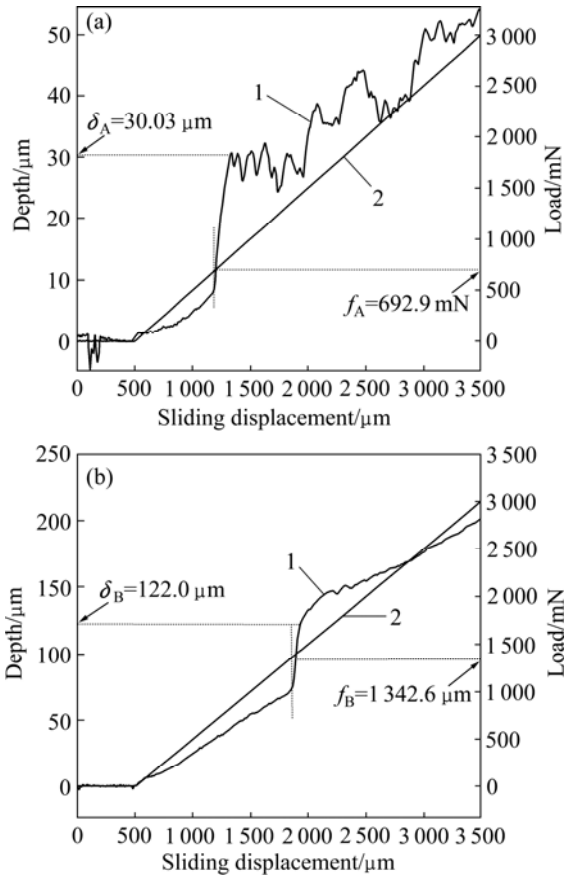

Fig.4 Relationships among depth, load and sliding displacement of repeated direct sol-gel(a) and composite coatings(b)

proportional loading plot as curve 2. The critical point of the coating failure is detected by an abrupt change with a continual fluctuation in the displacement of the probe, and the load at this point is defined as critical load for adhesive failure, which can be used as indication to evaluate the adhesive force between the coating and the substrate. The critical load represents the comprehensive capability of the coating to withstand exotic destruction depending on the characteristics of coating, substrate and interface. By this means, the critical loads of the two coatings are 692.9 mN for the repeated direct sol-gel and 1 342.6 mN for the composite coating, respectively. This obviously means that the adhesion force between the composite coating and the substrate is significantly higher than that for the repeated direct sol-gel coating, and this can be attributed to the different microstructures as well as the properties of the coatings. Since the cracks and the gaps between layers in the repeated direct sol-gel coating impose adverse influence on its adhesion strength, the coating is readily subjected to a failure under external force. But for the composite coating, the reinforcement of the Al_2O_3 filler in the layer as well as the crack-free structure endows the coating with an increased resistance to failure. The spinodal points in the scratch topography representing the reached bottom of the coating indicate the thickness of about 30 μm for the repeated direct sol-gel coating and about 122 μm for the composite coating. These values are in pronounced agreement with those results by SEM micrographs.

3.4 Corrosion resistance of coatings

Fig.5 presents the polarization curves of the repeated direct sol-gel and the composite coatings as well as the substrate. The derived electrochemical parameters can be seen in Table 1. The coated samples with elevated open circuit potentials (OCP) and lower corrosion current density indicate that the general corrosion resistance of the coated samples is fairly better than that of the substrate. It can also be seen from Fig.5 that the composite coating has a higher OCP and a reduced corrosion current density compared with that of the repeated direct sol-gel coating. It may be interpreted that the crack-free composite coating is thicker, whereas the repeated direct sol-gel coating is thinner and has more cracks. It should be noted that the increased thickness of the composite coating undoubtedly contributes much to improving the corrosion resistance of magnesium alloy.

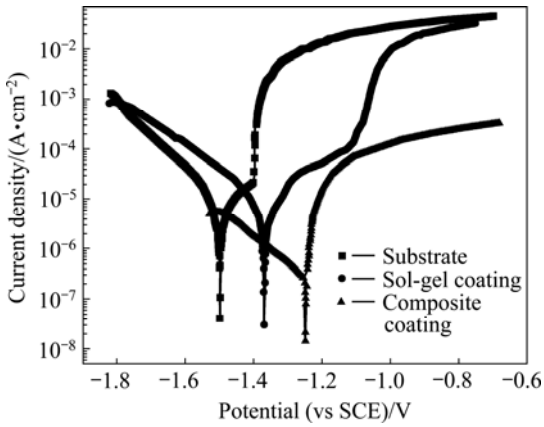

Fig.5 Polarization curves of direct sol-gel, composite coatings and substrate

Table 1 Corrosion current density and corrosion potential of coated samples and substrate

Material	Corrosion current density/(A·cm^{-2})	Corrosion potential (vs SCE)/V
Substrate	1.19×10^{-5}	−1.50
Direct sol-gel coating	1.07×10^{-5}	−1.37
Composite coating	2.70×10^{-7}	−1.25

4 Discussion

The repeated direct sol-gel deposition on the same substrate can achieve thicker coatings at the expense of leaving cracks and interlayer gaps which affect the

coating adhesion, strength as well as corrosion property. The composite coating with thickness up to 100 μm achieved a structural integrity and low level of cracks. It is illustrated that the dispersed Al_2O_3 ceramic particles are bonded with the gel phase. The composite coatings still need a relatively high temperature to gain enough strength and hardness and eliminate porosity. But for magnesium alloy, the maximum curing temperature should not exceed about 300 ˚C. The alumina phosphate-bonded ceramic phase is produced through phosphating treatment where a chemical reaction between alumina gel and the phosphate is initiated. The chemical bonding through phosphating eliminates the porosity and enhances the densification of the coating effectively. Therefore, its mechanical properties are improved. It seems that the visible pores distributing in the composite coating (see Fig.2(c)) are probably ascribed to the inadequate chemical bonding reaction.

In the composite coating, the chemical bonding reaction with derived aluminum phosphate, for example $Al(H_2PO_4)_3$, may be illustrated as[20−21]:

$$Al_2O_3+6H_3PO_4 \longrightarrow 2Al(H_2PO_4)_3+H_2O \quad (1)$$

$$Al(H_2PO_4)_3+H_2O \longleftrightarrow 2H_3PO_4+AlPO_4\cdot H_2O \quad (2)$$

For the composite method, the slurry has a high viscosity to form a thicker coating in one fabrication cycle rather than repeated deposition. The one-times process avoids forming layer cracks, which improves the adhesion to the substrate and increases the bonding strength. The ceramic bond system can absorb the thermal restrain upon heat treatment and reduce the formation of cracks. This kind of structure together with an increased thickness characterize that the coating has an improved anti-corrosion property. Hence, the thicker composite coating provides higher corrosion resistance by two orders of magnitude than the sol-gel coating.

5 Conclusions

1) The composite coating can be deposited as a more uniform and thicker crack free layer than that of repeated direct sol-gel coating.

2) The composite coating has an improved adhesion to the substrate compared with that of the repeated direct sol-gel coating.

3) The composite coating has an eminent anti-corrosion performance compared with that of the repeated direct sol-gel coating.

References

[1] GRAY J E, LUAN B. Protective coatings on magnesium and its alloys: A critical review [J]. J Alloys Compd, 2002, 336(1/2): 88−113.

[2] ZENG Rong-chang, HANG Jin, HUANG Wei-jiu, DIETZEL W, KAINER K U, BLAWERT C, KE Wei. Review of studies on corrosion of magnesium alloys [J]. Trans Nonferrous Met Soc China, 2006, 16: s763−s771.

[3] NATARAJAN S, RAVIKIRAN V. Evaluation of electrochemical and surface characteristics of conversion coatings on ZM21 magnesium alloy [J]. Surf Eng, 2006, 22(4): 287−293.

[4] ZENG Rong-chang, LAN Zi-dong, CHEN Jun, MO Xian-hua, HAN En-hou. Progress of chemical conversion coatings on magnesium alloys [J]. The Chinese Journal of Nonferrous Metal, 2009, 19(3): 397−404. (in Chinese)

[5] LI Ling-ling, CHENG Ying-liang, WANG Hui-min, ZHANG Zhao. Anodization of AZ91 magnesium alloy in alkaline solution containing silicate and corrosion properties of anodized films [J]. Trans Nonferrous Met Soc China, 2008, 18(3): 722−727.

[6] CHEN Chuang-zhong, DONG Qing, WANG Dian-gong. Microstructure and element distribution of ceramic-like coatings on the AZ91 alloy by micro-arc oxidation [J]. Surf Rev Lett, 2006, 13(1): 63−68.

[7] BOHNE Y, MANOVA D, BLAWERT C, STORMER M, DIETZEL W, MANDL S. Deposition and properties of novel microcrystalline Mg alloy coatings [J]. Surf Eng, 2007, 23(5): 339−343.

[8] ANGELINI E, GRASSINI S, ROSALBINO F, FRACASSI F, D'AGOSTINO R. Electrochemical impedance spectroscopy evaluation of the corrosion behavior of Mg alloy coated with PECVD organosilicon thin film [J]. Prog Org Coat, 2003, 46(2): 107−111.

[9] TIAN X B, WEI CB, YANG S Q, FU R K Y, CHU P K. Corrosion resistance improvement of magnesium alloy using nitrogen plasma ion implantation [J]. Surf Coat Technol, 2005, 198(1/3): 454−458.

[10] ZHANG Jin, SUN Zi-fu. Research on magnesium alloy AZ91D surface coating by metallizing aluminum [J]. China Mechanical Engineering, 2002, 13(23): 2057−2058. (in Chinese)

[11] TAMAR Y, MANDLER D. Corrosion inhibition of magnesium by combined zirconia silica sol-gel films [J]. Electrochim Acta, 2008, 53: 5118−5127

[12] KOBAYASHI Y, ISHIZAKA T, KUROKAWA Y. Preparation of alumina films by the sol-gel method [J]. J Mater Sci, 2005, 40: 263−283.

[13] ZHONG Xian-kang, LI Qing, CHEN Bo, WANG Ju-ping, HU Jun-ying, HU Wei. Effect of sintering temperature on corrosion properties of sol-gel based Al_2O_3 coatings on pre-treated AZ91D magnesium alloy [J]. Corros Sci, 2009, 51: 2950−2958.

[14] LI Qing, ZHONG Xiang-kang, HU Jun-ying, KANG Wei. Preparation and corrosion resistance studies of zirconia coating on fluorinated AZ91D magnesium alloy [J]. Prog Org Coat, 2008, 63: 222−227.

[15] FEIL F, FURBETH W, SCHUTZE M. Nanoparticle based inorganic coatings for corrosion protection of magnesium alloys [J]. Surf Eng, 2008, 24(3): 198−203.

[16] PHANI A R, GAMMEL F J, HACK T. Structural, mechanical and corrosion resistance properties of Al_2O_3-CeO_2 nanocomposites in silica matrix on Mg alloys [J]. Surf Coat Technol, 2006, 201: 3299−3306.

[17] GALIO A F, LAMAKA S V, ZHELUDKEVICH M L, DICK L F P, MULLER I L, FERREIRA M G S. Inhibitor-doped sol-gel coatings for corrosion protection of magnesium alloy AZ31 [J]. Surf Coat Technol, 2010, 204: 1479−1486.

[18] HUBERT T, SCHWARZ J, OERTEL B. Sol-gel alumina coatings on stainless steel for wear protection [J]. J Sol-Gel Sci Technol, 2006, 38: 179−184.

[19] WILSON S, HAWTHORNE H M, YANG Q, TROCZYNSKI T. Scale effects in abrasive wear of composite sol-gel alumina coated light alloys [J]. Wear, 2001, 251: 1042−1050.

[20] TROCZYNSKI T, YANG Q. Chemically bonded composite sol-gel alumina coatings [J]. J Am Ceram Soc, 2005, 88(9): 2420−2423.

[21] HAWTHORNE H M, NEVILLE A, TROCZYNSKI T, HU X, THAMMACHART M, XIE Y, FU J, YANG Q. Characterization of chemically bonded composite sol-gel based alumina coatings on steel substrates [J]. Surf Coat Technol, 2004, 176(2): 243−252.

(Edited by LI Yan-hong)